Corrosion effects on high-cycle fatigue lifetime and fracture behavior for heat-treated aluminum-matrix nano-clay-composite compared to piston aluminum alloy

Hanieh Aroo
Semnan University
Mohammad Azadi (m.azadi.1983@gmail.com)
Semnan University https://orcid.org/0000-0001-8686-8705
Mahboobeh Azadi
Semnan University

Research Article

Keywords: Corrosion effect, Aluminum alloy, Nano-clay-composite, High-cycle fatigue lifetime, Fracture behavior, Heat treatment

Posted Date: April 5th, 2021

DOI: https://doi.org/10.21203/rs.3.rs-323029/v1

Version of Record: A version of this preprint was published at Silicon on May 18th, 2021. See the published version at https://doi.org/10.1007/s12633-021-01129-w.

Abstract

In this research, the corrosion effect has been investigated on the high-cycle fatigue lifetime and the fracture behavior for the heat-treated aluminum-matrix nano-clay-composite and piston aluminum alloys. For this objective, after fabricating stir-casted nano-clay-composite, standard samples were machined and rotary bending fatigue tests were performed. To study the corrosion effect, some specimens were corroded in in the 0.00235% H_2SO_4 solution after 200 hours and then, they were tested under cyclic bending loading. Due to increase in the hardness by adding nano-clay particles and the heat treatment, higher fatigue strength occurred, compared to the base material. Nano-clay particles shortened the fatigue lifetime; however, this effect was less in the corrosion-fatigue lifetime. Moreover, the failure mechanism was the brittle fracture behavior due to the observation of quasi-cleavage and cleavage marks.

Introduction

Advantages of aluminum-silicon alloys are clear enough for the application in engine and automotive components. Such these benefits are related to the casting behavior, the density, the wear lifetime and the fatigue lifetime, either at moderate temperatures [1–3]. Therefore, understanding material behaviors could be important for designers. However, as a problem in diesel engines, components in the combustion chamber have been exposed to cyclic loadings under environmental effects. These factors contain high temperatures and corrosive fluids, which decrease the material lifetime. In order to improve material characteristics, the heat treatment process could be used by engineers as a common solution. Moreover, based on an innovative approach, nano-particles-reinforced aluminum-matrix composites have been fabricated in the literature [2–3], by adding nano-particles besides the heat-treatment. These reinforcements could increase the material lifetime.

In following paragraphs, a literature review could be seen for fatigue properties of aluminum alloys [4–13] and aluminum-matrix composites [14–17]. In addition, some other articles [18–37] have been reviewed for corrosion-fatigue properties of aluminum alloys.

Ueno et al. [4] studied fatigue properties of Al-Si-Cu alloys in ambient air and vacuum environments. As an expectation, the fatigue lifetime in the vacuum were always longer than that the air. Teranishi et al. [5] indicated that under cyclic loading and in the low-cycle fatigue regime, cracking generally started by the fracture of Si particles, in the Al-Si-Mg aluminum alloy. That was due to the equivalent plastic strain, concentrated near Si particles. Azadi [6] demonstrated no significant influence on the thermo-mechanical fatigue lifetime of the A356.0 alloy, using the heat treatment. The reason was due to over-ageing at high temperatures. Moffat et al. [7] studied the influence of the silicon content on the long crack fatigue of piston aluminum alloys at high temperatures. They found that the Si phase had an inverse effect on the fatigue strength. Mbuya et al. [8] investigated the fatigue crack growth behavior in as-cast and hot-pressed aluminum alloys. Their results illustrated that pressing reduced the porosity, which effectively enhanced the ductility and subsequently, improved the fatigue crack growth resistance.

Mbuya et al. [9] analyzed the fatigue crack initiation and the stress-lifetime response of cast aluminum alloys, after over-ageing at 260℃ for 100 hours. They depicted that hipping had no effects on the fatigue behavior of Al7Si-Sr. However, hipping improved the fatigue resistance of Al0.7Si, due to lower porosity. Nicoletto et al. [10] checked high-temperature fatigue behaviors of eutectic Al-Si alloys, used in the engine piston. They found higher fatigue strength at room temperature for the hot forged alloy. By increasing the temperature, the fatigue strength decreased significantly at 250℃. Mbuya and Reed [11] studied the short fatigue crack growth behavior in Al-Si alloys. Their results illustrated that intermetallic particles and eutectic Al-Si regions had an effective role on the crack path and the growth rate. Wang et al. [12] presented low-cycle fatigue behaviors and the lifetime estimation of the piston aluminum alloy at high temperatures. They indicated that fatigue cracks usually initiated near Si phases. When the temperature increased, ductile tearing occurred through micro-cracks. Rezanezhad et al [13] demonstrated the heat treatment changed the Si distribution and its size. Therefore, the high-cycle bending fatigue lifetime surprisingly enhanced by the process of heat treating.

For the second category of the literature review on composites, Myriounis et al. [14] reported the fatigue behavior of SiCp particulate-reinforced A359 aluminum-matrix composites. Their results illustrated that the fatigue strength had dependency on the heat treatment. The reason was linked to the microstructure and good matrix-particulate interfacial properties. Divagar et al. [15] investigated the impact of the nano-sized particles on the fatigue lifetime of the AA7075-T651 aluminum alloy. They demonstrated that the nano-composite had higher fatigue strength than that of the base metal. The optimized value for SiC and Al_2O_3 nano-particles was 10% and 5% respectively. Raju et al. [16] evaluated the fatigue lifetime of the nano-composite, fabricated from the Al2024 aluminum alloy and Al_2O_3 nano-particles, using the stir casting technique. They revealed that based on the stress-lifetime curve, the nano-composite fatigue behavior was better than that in the base material. Azadi et al. [17] studied low-cycle fatigue properties at elevated temperatures in piston aluminum alloys, both with and without reinforcements, the heat treatment nano-clay particles. They obtained that the reinforcement influence was not significant on the low-temperature fatigue lifetime. Moreover, at 300 ℃, the fatigue lifetime of aluminum alloys decreased effectively using reinforcements.

In the third category, a literature review was done for corrosion-fatigue tests. Chlistovsky et al. [18] presented the corrosion-fatigue behavior of the 7075-T651 aluminum alloy under cyclic over-loadings. However, they showed that the corrosion-fatigue phenomenon did not have a large influence on the fatigue lifetime in the low-cycle fatigue regime (high stress levels. It was depicted from fractographic evidences that the decrease in the lifetime under high-cycle fatigue regims was due to premature the crack initiation, which was from corrosion pits, formed on the surface of the sample. Galyon Dorman and Lee [19] studied the chromate primer effect on the corrosion-fatigue behavior in the AA7075-T651 aluminum alloy. Their tests in the pure water suggested that the ratio of chloride to chromate had influences on the efficacy of chromate. Mhaede [20] investigated the influence of ball-burnishing and shot peening on fatigue and corrosion-fatigue performances of the AA7075-T73 alloy. Their results illustrated that the corrosion effectively decreased the fatigue lifetime and such surface treatments enhanced the corrosion-fatigue lifetime. Meng et al. [21] measured the corrosion-fatigue crack growth rate behavior in the 7075 aluminum alloy. They proved that the crack growth rate accelerated when the corrosion solution concentration increased. Moreover, the crack growth rate enhanced, when the load frequency decreased, due to the longer corrosion exposure of the specimen. Corrosion pits were responsible for the acceleration of the crack growth rate. Moreover, around the crack-tip, corrosion pits might act as physical defects and the stress concentration. Abdulstaar et al. [22] investigated influences of bulk and surface severe plastic deformations on fatigue, corrosion and corrosion-fatigue behaviors of the AA5083 alloy. Their result demonstrated that the fatigue lifetime was significantly increased by shot peening and ball-burnishing.

Laurino et al. [23] studied the corrosion effect in the NaCl solution on the fatigue lifetime and fracture mechanisms of 6101 aluminum wires. They claimed that the pre-corrosion heat treatment led to a decrease in the number of cycles to failure, due to premature the crack initiation on corrosion defects. Chemin et al. [24] investigated the corrosion-fatigue crack growth of the 7475-T7351 aluminum alloy in the air and the saline environment. Their results demonstrated that the fatigue crack propagation lifetime of samples in the saline was longer than ones in the air. Guerin et al. [25] depicted the fatigue behavior of the 2050 aluminum-copper-lithium alloy in the air for healthy and pre-corroded samples in the 0.7 NaCl solution. They found that the fatigue lifetime in the air on pre-corroded samples implied an effective decrease due to the presence of corrosion defects. The T34 metallurgical state had more influences on the corrosion-fatigue behavior based on the increased propagation of the inter-granular corrosion. Hu et al. [26] presented a continuum damage mechanics technique coupled with the pit evolution model for the corrosion-fatigue behavior of the aluminum alloy. They showed an evident for the interaction between the fatigue damage evolution and the pit growth. During loadings, the accumulated fatigue damage degraded material properties around pits and then, resulted in the stress redistribution. Under higher stress levels, corrosion-fatigue lives decreased effectively. Wang et al. [27] found a modified Trantina-Johnson model to predict the corrosion-fatigue crack growth behavior for evaluating residual lives of aluminum alloys. Their models had a good correlation with experimental results.

Priet et al. [28] investigated the effect of usual hydrothermal sealing and presented an innovating sealing process on fatigue properties of the anodized AA2024 alloy in the air, for both as-prepared and pre-corroded specimens, by the salt-spray or continuous immersions. The fatigue lifetime in the air on pre-corroded samples revealed that anodized samples had a decrease than anodized and sealed specimens due to lower corrosion resistance. Chen et al. [29] studied the effect of the pre-deformation on pre-corrosion multiaxial fatigue behaviors of the 2024-T4 aluminum alloy. With the same pre-deformation level, the pre-corrosion multiaxial fatigue lifetime decreased, when the pre-corrosion time increased, due to pitting on the surface of specimens. Leon and Aghion [30] presented the effect of the surface roughness on the corrosion-fatigue performance of the AlSi10Mg alloy, fabricated by the selective laser melting. The obtained results indicated that the corrosion resistance and corrosion-fatigue lifetime improved after the polishing process, comparing to that of the unpolished specimen, due to cavities and other surface defects. Chen et al. [31] found multiaxial fatigue behaviors of the 2024-T4 aluminum alloy under different corrosion conditions in the NaCl solution. They demonstrated that when the pre-corrosion time increased, the multiaxial fatigue lifetime decreased due to corrosion pits. Increasing the pre-corrosion time led to have higher number and larger size of pits. Arunachalam et al. [32] depicted the effect of electrical discharge machining on corrosion and corrosion-fatigue phenomena aluminum alloys. They revealed that the corrosion potential of the process was greater, compared to milled surface of the material, due to act as a galvanic couple to an adjacent bulk surface.

Ye et al. [33] studied the effect of combined shot peening and the plasma electrolytic oxidation on the fatigue behavior of the 7A85 aluminum alloy in air and 3.5% NaCl solutions. Their results indicated that one surface treatment reduced the corrosion-fatigue lifetime. However, the corrosion-fatigue performance improved by both treatments due to the residual compressive stress field induced by the shot peening process. Chen et al. [34] investigated the influence of alternate corrosion factors on the multiaxial low-cycle fatigue lifetime of the 2024-T4 aluminum alloy. They illustrated a reduction tendency of the lifetime by increasing of the corrosion time, the temperature and the corrosion solution flow rate, as also the decrease of the pH value. Rodriguez et al. [35] founded corrosion effects on the fatigue behavior of dissimilar friction stir welding of high-strength AA6061-to-AA7050 aluminum alloys. Their results showed a localized corrosion damage in the thermo-mechanically affected and heat-affected zones due to pitting, pit clustering, and the exfoliation. Then, they observed a decrease in the fatigue lifetime with the evidence of the crack initiation at corrosion defects. Moreover, they claimed that the lifetime was nearly independent of the exposure time due to the incubation time. Mishra [36] investigated the pre-corrosion influence on mechanical properties and the fatigue lifetime of the 8011 aluminum alloy. They showed that due to corrosion pits on the surface, the ultimate tensile strength properties decreased but not effectively. However, the fatigue strength decreased significantly. Huang et al. [37] presented the equivalent crack size model for the pre-corrosion-fatigue lifetime prediction of the 7075-T6 aluminum alloy. They correlated parameters between equivalent cracks and corrosion pits, using the Pearson correlation analysis.

Based on the mentioned literature review, the research on corrosion-fatigue properties of heat-treated aluminum-matrix nano-composites has been so limited or non-existed until now. Moreover, the corrosive environment (the acid type) for the combustion engine applications was not investigated by researchers for the evaluation of fatigue properties. Therefore, in this article, the corrosion effect on the high-cycle fatigue lifetime and the fracture behavior for the heat-treated aluminum-matrix nano-composite was studied and then also compared to the base material. For this target, rotary bending fatigue testing was done on machined standard samples, fabricated from piston aluminum-silicon alloys, with and without nano-clay particles, both for as-prepared and pre-corroded samples.

Experimental Works

In this research, the studied material was aluminum-silicon (AlSi12CuNiMg) alloy. The application of this material is in combustion engine pistons in the automotive industry. The chemical composition of the initial material depicts in Table 1. Then, to reinforce the material, nano-clay particles (type: montmorillonite K10) were used in the aluminum-matrix. The weight percent of nano-clay particles was considered as 1% based on the literature [17, 38]. Moreover, the chemical composition of nano-clay particles shows in Table 2. Based on the literature [3], pre-heating of nano-particles caused to a superior wetting in the aluminum-silicon melt than that which made by the ball-milling process. To fabricate initial materials, nano-clay particles were firstly pre-heated at 400°C [39] and then, were added into the aluminum melt by the stir, with the amount of 2 gr. This work was done to have a better melt quality and also to eliminate any gas accumulations in the aluminum melt [17, 40].

Table 1
The aluminum alloy chemical composition

Element	Al	Si	Fe	Cu	Mg	Ni	Zn	Mn
Amount (%)	Base	12.70	0.56	1.16	1.00	0.80	0.16	0.12

Table 2
The nano-clay chemical composition

Element	SiO_2	Al_2O_3	LOI	Fe_2O_3	MgO	CaO	Na_2O	K_2O	TiO_2
Amount (%)	50.95	19.60	15.45	5.62	3.29	1.97	0.97	0.86	0.62

The fabrication technique for the piston aluminum-silicon alloy for fatigue testing was the gravity casting approach. The production method for the aluminum-matrix nano-composite was the stir-casting method. For the objective of fabricating standard cylindrical samples, aluminum ingots were firstly melted. Then, the aluminum melt was held for 2 hours at 700°C. The casting process of all initial samples was about 5 min, one by one. After waiting for 20 min, nano-clay particles were added the melt. Moreover, all initial specimens were air-quenched. Then, fatigue standard samples were machined from casted initial specimens. The geometry depicts in Fig. 1. After machining, nano-clay-composite samples were also heat-treated at 500°C for 1 hour, water-quenched and aged at 200°C for 5 hours [41].

Based on the literature [13], the heat treatment could change the Si distribution and the Si size in the aluminum-matrix in aluminum-silicon alloy. Then also, the hardness increases effectively and consequently, the stress-controlled fatigue lifetime increases. Sasaki and Takahashi [42] showed that precipitation hardening occurred after T6 heat treating, which was higher than T4, T5, T7, T8 and T9 heat treatments.

Fatigue testing including cyclic bending was carried out under the fully-reversed condition ($R = -1$), based on the ISO-1143 standard [43]. This experiment was done by the rotary bending fatigue testing equipment (SFT-600 from SANTAM Company). During cyclic bending loading, the stress value was controlled. Therefore, in each test, the stress amplitude was constant in the regime of the high-cycle fatigue. However, each stress level was tested for at least 3 times for the repeatability of testing. The loading frequency was 100 (Hz) at the room temperature. Such a loading case could be found during working conditions of the vehicle engine. In addition, the fatigue lifetime of the run-out sample was limited to 2×10^6 cycles [44].

For the stress-lifetime curve, the following formulation could be utilized [13],

$$\sigma_a = \acute{\sigma}_f \left(2N_f\right)^b \quad (1)$$

Where N_f is the fatigue lifetime and σ_a is the stress amplitude. Moreover, material constants include b as the fatigue strength exponent and $\acute{\sigma}_f$ as the fatigue strength coefficient [13].

For corrosion-fatigue tests, the samples were pre-corroded at 0.00235% H_2SO_4, which was selected based on the maximum sulfur content in the gasoline fuel in diesel engines. The time duration for the corrosion was about 200 hours [41]. The specimens after the pre-corrosion could be seen in Figure 1.

To study the fracture surface and to find failure mechanisms during cyclic loadings, the field-emission scanning electron microscopy (FE-SEM) was used based on the MIRA TESCAN model, in the secondary mode. In addition, the energy dispersive X-ray spectroscopy (EDS) map was utilized to indicate the material chemical composition on the fracture surface od samples. For this objective, the back-scattered mode of FE-SEM images were taken. Moreover, the other objective of the back-scattered FE-SEM image was to find the distribution of nano-clay particles in the aluminum matrix. Then also, to find the effect of the heat treatment and nano-clay particles, before testing, microstructures were examined by the optical microscopy (OM), using the Olympus model. For such objective, a polishing process was firstly performed on specimens and then, a Keller etchant (solution including 1.5 ml HCL, 2.5 ml HNO_3, 1.0 ml HF and 95 ml H_2O) was utilized [1,3,38,45].

For a better presentation of obtained results, an explanation of the abbreviations used for the materials is given in Table 3 for samples and testing types. The last experiment was the harness test, which was performed by the Brinell method and the macro-hardness type. For this objective, a bullet with a diameter of 2.5 mm and an applied force of 31.25 kilograms Force was used. In addition, the duration of the force was 10-15 seconds.

Table 3
The explanation of the abbreviations used for the materials

Abbreviations	Explanation
AlSi_N0_T0	Aluminum-silicon alloy
AlSi_N1_T0	Aluminum-silicon alloy, reinforced with nano-particles
AlSi_N1_T6	Aluminum-silicon alloy, reinforced with nano-particles and the heat-treatment
PF	Pure bending fatigue testing
CF	Corrosion-fatigue testing

Results And Discussions

As the first result, hardness test results are given. A comparative diagram of the hardness test results with the deviation standard is shown in Fig. 2. As it could be seen, the hardness of the AlSi_N0_T0, AlSi_N1_T0 and AlSi_N1_T6 was 86, 121 and 122 BH, respectively. It could be concluded that by adding nano-clay particles, the hardness increased significantly as 40.6%, and also by reinforcing with nano-clay particles and also the heat treatment, the hardness increased as 41.8%.

According to the literature [13, 40], which was performed on aluminum-silicon piston alloys, by applying the heat treatment process and adding nano-silica particles, the hardness of the alloy increased by 36% and 18%, respectively, compared to the base alloy. Jang et al. [39] also reinforced aluminum alloys using nano-alumina particles. They found that the hardness of the aluminum alloy increased by 20.7% with the addition of nano-particles. These results could confirm the results of this study.

As the second result, the OM images of aluminum-silicon alloys, unreinforced and reinforced with nano-particles and also reinforced with nano-particles and the heat treatment, before fatigue testing, could be seen in Fig. 3. All specimens contained the same phases; however, the size and the morphology of phases were different. These different phases included the main phase, which was α-Al as the matrix with the light-gray color. Moreover, the second phase was Si, with two morphologies. One of the shapes was a blocky form, including polyhedral crystals, and the other one was a flaky or needle-like morphology that was homogeneously distributed in the matrix. Zainon et al. [46] reported that there were two Si phase types, including the flake-like form and also the coarse primary phase of Si particles. The black-colored area in the matrix was (Al,Ni) intermetallic phase. Another intermetallic phase was also (Al,Cu) precipitate which was seen in the brown-color area. Such obtained results were also seen in the literature [1, 3, 47–49].

As shown in Fig. 3, the heat treatment caused an insignificant increase in the amount of the (Al,Ni) intermetallic phase in the aluminum-matrix. Such phenomena could enhance and improve the strength of the material [38]. In addition, the shape of the Si phase changed after the heat treatment. It seemed that the thickness of Si precipitates increased.

Adding nano-particles to the aluminum-matrix changed the morphology of the (Al,Ni) intermetallic phase, into the flaky shape, as shown in Fig. 3. Besides, the size of the Si phase decreased by presence of nano-particles. As a result, the ratio of the diameter to the length for intermetallic phases and the Si phase decreased significantly. Similar results were reported in the literature [12, 49]. In addition, Issa et al. [50] found a decrease in the grain size, when brittle ceramic nano-particles reinforced the matrix. More details of these microstructures including FE-SEM images were found in previous studies [1, 3]. Azadi et al. [17, 38] and Sharifi et al. [53] showed that by the presence of the reinforcement (nano-particles plus the heat treatment), the change in the Si morphology was significant and seemed to be the needle-shape and also the block shape. Due to the reinforcement, the Si phase percentage enhanced as 8%. The root cause was the nano-clay chemical composition, including about 50% SiO_2. Moreover, the Si phase area enhanced as 9% by the reinforcement. Such changes in the material microstructure could shorten the fatigue lifetime and also decrease mechanical properties, as also reported in [17, 42, 51–52]. Besides, a decrease could be observed in the intermetallic percentage and the intermetallic area, as 21% and 15% respectively, in the reinforced material [17].

Obtained results from fatigue and corrosion-fatigue testing as the stress-lifetime (S-N) curve for piston aluminum alloys could be seen in Figs. 4 and 5. In Fig. 4, the curves were compared to different type of materials and in Fig. 5, fatigue and corrosion-fatigue lifetimes of different alloys were compared. Moreover, the S-N curve included the stress amplitude versus the high-cycle fatigue lifetime. According to these figures, all experimental data were presented plus curve fitting. In addition, averaged experimental data points were also drawn in a logarithmic scale for the fatigue lifetime at each stress level. Based on these results and also curve fitting, fatigue and corrosion-fatigue properties of studied materials were obtained and are shown in Table 4.

Table 4: Fatigue properties of studied materials based on all data and averaged values

Materials	Conditions	All data			Averaged data		
		b	$\acute{\sigma}_f$ (MPa)	R^2	b	$\acute{\sigma}_f$ (MPa)	R^2
AlSi_N0_T0	As-prepared	-0.600	1502.103	0.9255	-0.647	1811.340	0.9882
AlSi_N1_T0	As-prepared	-0.391	643.576	0.8549	-0.403	677.954	0.8730
AlSi_N1_T6	As-prepared	-0.756	3050.406	0.7319	--0.856	4616.363	0.8820
AlSi_N0_T0	As-corroded	-0.504	909.285	0.8719	-0.528	1007.163	0.9995
AlSi_N1_T0	As-corroded	-0.375	513.334	0.9324	-0.384	534.687	0.9808
AlSi_N1_T6	As-corroded	-0.685	1863.803	0.8260	-0.765	2500.345	0.9002

Due to higher hardness of AlSi_N1_T6 compared to the base piston alloy, it could be concluded that the fatigue strength of the material increased. In addition, according to Fig. 4, it could be seen that the corrosion-fatigue lifetime of aluminum-silicon alloys reinforced with nano-particles and the heat treatment also increased, compared to the aluminum-silicon alloy, under high stress levels. However, at low stress levels, this behavior was not observed and the fatigue lifetimes were almost similar for different types of the material. Such a result was shown by Rezanezhad et al. [13]. They indicated an improvement in the high-cycle fatigue lifetime, using the heat treatment, which was lower under the lowest stress level than that under the highest stress level.

Based on Fig. 4, the use of nano-particles alone, under high and low stress ranges reduced both the fatigue lifetime and the corrosion-fatigue lifetime of the material. Based on averaged values, the fatigue lifetime increased by the heat treatment and the nano-particles reinforcement as 128% under 210 MPa and through the low-cycle fatigue regime. This value for the corrosion-fatigue phenomenon was 114%. In other words, the corrosion phenomenon reduced such an improvement. The reduction of the fatigue lifetime and the corrosion-fatigue lifetime under 210 MPa was 81% and 76% respectively, by adding nano-clay particles. It means that nano-particles decreased the negative influence on the fatigue lifetime in the corrosive environment. However, in general, the effect of the nano-particles reinforcement was negative on the fatigue properties of the material. These fatigue and corrosion-fatigue behaviors under 120 MPa or within the high-cycle fatigue regime were similar for various materials.

Myriounis et al. [14] investigated the fatigue properties in SiC-particulate-reinforced A359 aluminum-matrix composites. They implied increases in the fatigue strength due to the use of these particles. And also, they showed the fatigue strength strongly depended on the heat treatment. Such a result could be also seen in this report and the effect of the heat treatment was higher than the reinforcement influence. For the effect of nano-particles, Divagar et al. [15] introduced a metal matrix nano-composite, consisting of AA7075-T651 + SiC-10%+Al_2O_3-5%, which exhibited 12% higher fatigue performance than the base material and also other composites. Raju et al. [16] observed that the fatigue properties of the composite (Al2024/Al_2O_3), which was slightly better than that of the base metal. Azadi et al. [17] showed that the nano-clay particles reinforcement had no significant effect on the low-cycle fatigue lifetime of aluminum-silicon alloys. These slight improvements or no influences of nano-particles on the fatigue lifetime could be also seen in this article, which indicated an agreement.

To compare fatigue and corrosion-fatigue lifetimes in Fig. 5, it is inferred that the corrosion-fatigue lifetime of all three alloys was less than the fatigue lifetime. In other words, the corrosion phenomenon reduced the fatigue lifetime of all samples. This was due to the surface defects (such as pits) caused by corrosion reactions. Similar result was presented by Guerin et al. [25] for the 2050 aluminum-copper-lithium alloy, which was pre-corroded in the 0.7 NaCl solution. The fatigue lifetime of pre-corroded specimens revealed a significant decrease compared to other samples, due to the presence of corrosion defects. This reduction could be observed as a shift in the curve-fitted lines. In other words, the fatigue strength coefficient reduced as 39%, 20% and 39% respectively for AlSi_N0_T0, AlSi_N1_T0 and AlSi_N1_T6 specimens. Chen et al. [29] illustrated that for the 2024-T4 aluminum alloy, the pre-corrosion process decreased the fatigue lifetime. Mishra [36] reported that the pre-corrosion phenomenon created corrosion pits on the surface of the 8011 aluminum alloy after the 100 hours. This led to initiate the crack and also to decrease the fatigue lifetime. He demonstrated when the bending stress was 120 MPa, the lifetime of the un-corroded specimen was twice of the corroded specimen. In this research, after 200 hours pre-corrosion, at the same value of the bending stress, the fatigue lifetime of the un-corroded specimen was almost 2.8 times higher than the corroded ones. It should be noted that the arrangement of weight losses after 200 hours of the corrosion time was AlSi_N1_T0, AlSi_N0_T0 and AlSi_N1_T6 samples [41].

To find the failure mechanism, FE-SEM images of the fracture surface for aluminum-silicon alloys under 150 MPa stress are shown in Fig. 6. As a first statement, the brittle fracture was seen according to the presence of cleavage and quasi-cleavage marks in all specimens under fatigue and corrosion-fatigue tests. Moreover, tear ridges, micro-cracks, and also broken intermetallics phases were also observed on the fracture surface of specimens, as also represented in the literature [13, 53–54]. As Zhang et al. [55] reported, when there was a brittle facture behavior in the material, the fatigue fracture of the piston aluminum alloy happened in a perpendicular direction to the force axis. In addition, at the specimen surface, the crack initiated usually near intermetallic phases.

Figure 6(b) indicated that the brittle region of the fractured surface was larger for specimens after the 200 hours corrosion than other specimens. It is believed that the reduced fatigue lifetime in corrosion-fatigue tests was due primarily to the formation of corrosion pits [18]. In addition, more defects including corrosion products such as hydrated aluminum oxides were found on the fracture surface. Such defects caused a reduction in the fatigue lifetime.

Based on OM and FESEM images, the small size of the silicon phase in the matrix caused longer fatigue lifetime, since these precipitates could be the sites for the stress concentration. In addition, when the size of the silicon phase or other intermetallic precipitates was small in the matrix, less corrosion attacks would be performed due to fewer micro-galvanic effect [56]. Therefore, in the sample reinforced with nano-clay particles and the heat treatment, the fatigue and corrosion-fatigue lifetimes were longer than other samples.

As shown in Fig. 6(a), the morphology of the cavities created in samples was different. The cavities were observed in a shallow-form in the specimen with nano-particles and also the heat treatment. As a note, similar results were mentioned in the reference [57], where was performed on the 6061 aluminum alloy, the morphology of the cavity was affected by the addition of silicon carbide particles into the 6061 aluminum alloy matrix. In this system, irregular holes were expanded in the composite, while much smaller circular holes were formed in the aluminum alloy [57].

Based on the results of Figs. 6 (b), the amount of cavities and their interconnections for the sample with nano-particles increased, compared to the sample without nano-particles. This indicated an increase in the corrosion rate. It is noteworthy that after increasing the immersion time, the effect of the presence of the micro-galvanic effect decreased. Therefore, this may be the reason for the change in the corrosion rate behavior of the sample with and without nano-particles over the time. Such a result represented in the literature [41].

According to Fig. 6, in the sample with shorter fatigue lifetime, more and large cracks were seen on the slip plates. However, in the sample with longer fatigue lifetime, more holes were seen, which illustrated that in the sample with shorter fatigue lifetime, a more brittle fracture behavior occurred.

The EDX map after fatigue and corrosion-fatigue testing are shown in Figs. 7 and 8. As a result from Figs. 7 and 8, the failure mechanism included Si and intermetallics phases in all studied materials. This was due to this fact that these precipitates could cause the site for the micro-cracks initiation. Li et al. [58] illustrated that cracks and also the final fracture were near Si phases and intermetallics phases. In other words, the aluminum-matrix was not a potential region for cracking. According to Figs. 7and 8, the amount of the oxygen element in corrosion-fatigue samples was more than that of the fatigue specimens. This could be due to corrosion reactions and the formation of holes on the surface. In this situation, the corrosive solution penetrated through the cavities and the corrosion products would be created.

Conclusions

In this article, the corrosion influence on the high-cycle fatigue lifetime and the fracture behavior for the heat-treated aluminum-matrix nano-composite was compared to the base material and highlighted results could be shortened as follows,

- The hardness increased significantly in the piston aluminum alloy, by the addition of both nano-clay particles and the heat treatment. Moreover, the heat treatment effect was significant and changed the microstructure of the material, specially the (Al,Ni) intermetallic phase. In addition, nano-clay particles changed the morphology of this phase into the flaky shape. The Si phase size reduced by nano-particles.
- Higher hardness of heat-treated nano-composite led to higher fatigue strength, compared to the base material, especially through the low-cycle fatigue regime. However, the nano-particles effect was negative and the fatigue lifetime decreased.
- The corrosion effect in the 00235% H_2SO_4 solution after 200 hours, as expected, was negative on the fatigue lifetime of all specimens, due to surface defects and pits. This decrease was a shift in both low-cycle and high-cycle fatigue regimes.
- To find the failure mechanism, cleavage and quasi-cleavage marks were observed in all samples under fatigue and corrosion-fatigue tests, which showed the brittle fracture. The precipitates in the aluminum matrix were sites for the crack initiation.

Declarations

Funding statement

Authors tend to have special thanks to Motorsazi Pooya Neyestanak (MPN) Company, for supporting authors by providing initial materials, in addition to financial supports.

Conflict of Interest

For this research, there is no conflict of interest for all authors.

Author contributions

Hanieh Aroo: Software/ Formal analysis/ Investigation/ Resources/ Data Curation/ Writing - Original Draft / ***Mohammad Azadi:*** Conceptualization/ Methodology/ Validation/ Investigation/ Resources/ Writing - Review & Editing/ Visualization/ Supervision/ Project administration/ Funding acquisition / ***Mahboobeh Azadi:*** Methodology/ Validation/ Investigation/ Resources/ Writing - Original Draft

Availability of data and material

The data that support the findings of this study are available based on the request from the corresponding author. The experimental data are not publicly available due to restrictions and the privacy of research participants.

Compliance with ethical standards

This article does not contain any studies with human or animal subjects.

Consent to participate

Not applicable

Consent for Publication

Not applicable

References

[1] M. Azadi, S. Safarloo, F. Loghman, R. Rasouli, Microstructural and thermal properties of piston aluminum alloy reinforced by nano-particles, AIP Conference Proceedings, 1920 (2018) 020027

[2] M. Azadi, M. Zolfaghari, S. Rezanezhad, M. Azadi, Preparation of various aluminum matrix composites reinforcing by nanoparticles with different dispersion methods, Proceedings of Iran International Aluminum Conference, Tehran, Iran (2018)

[3] M. Azadi, M. Zolfaghari, S. Rezanezhad, M. Azadi, Effects of SiO_2 nano-particles on tribological and mechanical properties of aluminum matrix composites by different dispersion methods, Applied Physics A, 124(5) (2018) 377

[4] A. Ueno, S. Miyakawa, K. Yamada, T. Sugiyama, Fatigue behavior of die casting aluminum alloys in air and vacuum, Procedia Engineering, 2 (2010) 1937-1943

[5] M. Teranishia, O. Kuwazuru, Sh. Gennai, M. Kobayashi, H. Toda, Three-dimensional stress and strain around real shape Si particles in cast aluminum alloy under cyclic loading, Materials Science and Engineering A, 678 (2016) 273-285

[6] M. Azadi, Cyclic thermo-mechanical stress, strain and continuum damage behaviors in light alloys during fatigue lifetime considering heat treatment effect, International Journal of Fatigue, 99 (2017) 303-314

[7] A.J. Moffat, S. Barnes, B.G. Mellor, P.A.S. Reed, The effect of silicon content on long crack fatigue behavior of aluminum-silicon piston alloys at elevated temperature, International Journal of Fatigue, 27 (2005) 1564-1570

[8] T.O. Mbuya, I. Sinclair, A.J. Moffat, P.A.S. Reed, Micro-mechanisms of fatigue crack growth in cast aluminum piston alloys, International Journal of Fatigue, 42 (2012) 227-237

[9] T.O. Mbuya, I. Sinclair, A.J. Moffat, P.A.S. Reed, Analysis of fatigue crack initiation and S-N response of model cast aluminum piston alloys, Materials Science and Engineering A, 528 (2011) 7331-7340

[10] G. Nicoletto, E. Riva, A. Di Filippo, High temperature fatigue behavior of eutectic Al-Si alloys used for piston production, Procedia Engineering, 74 (2014) 157-160

[11] T.O. Mbuya, P.A.S. Reed, Micro mechanisms of short fatigue crack growth in an Al-Si piston alloy, Materials Science and Engineering A, 612 (2014) 302-309

[12] M. Wang, J.C. Pang, S.X. Li, Z.F. Zhang, Low-cycle fatigue properties and life prediction of Al-Si piston alloy at elevated temperature, Materials Science and Engineering A, 704 (2017) 480-492

[13] S. Rezanezhad, M. Azadi, M. Azadi, Influence of heat treatment on high-cycle fatigue and fracture behaviors of piston aluminum alloy under fully-reversed cyclic bending, Metals and Materials International, (2019)

[14] D. Myriounis, T. Matikas, S. Hasan, Fatigue behavior of SiC particulate-reinforced A359 aluminum matrix composites, Strain, 48 (2012) 333-341

[15] S. Divagar, M. Vigneshwar, S. Selvamani, Impacts of nano particles on fatigue strength of aluminum-based metal matrix composites for aerospace, Materials Today: Proceedings, 3 (2016) 3734-3739

[16] P.R.M. Raju, S. Rajesh, K.S.R. Raju, and V.R. Raju, Evaluation of fatigue life of Al2024/Al2O3 particulate nano composite fabricated using stir casting technique, Materials Today: Proceedings, 4 (2017) 3188-3196

[17] M. Azadi, H. Bahmanabadi, F. Gruen, G. Winter, Evaluation of tensile and low-cycle fatigue properties at elevated temperatures in piston aluminum-silicon alloys with and without nano-clay particles and heat treatment, Materials Science and Engineering A, 788 (2020) 139497

[18] R.M. Chlistovsky, P.J. Heffernan, D.L. DuQuesnay, Corrosion-fatigue behaviour of 7075-T651 aluminum alloy subjected to periodic overloads, International Journal of Fatigue, 29 (2007) 1941-1949

[19] S.E.G. Dorman, Y. Lee, Effect of chromate primer on hr in aluminum alloy 7075, Procedia Engineering, 10 (2011) 1220-1225

[20] M. Mhaede, Influence of surface treatments on surface layer properties, fatigue and corrosion fatigue performance of AA7075 T73, Materials and Design, 41 (2012) 61-66

[21] X. Meng, Z. Lin, F. Wang, Investigation on corrosion fatigue crack growth rate in 7075 aluminum alloy, Materials and Design, 51 (2013) 683-687

[22] M. Abdulstaar, M. Mhaede, M. Wollmann, L. Wagner, Investigating the effects of bulk and surface severe plastic deformation on the fatigue, corrosion behavior and corrosion fatigue of AA5083, Surface and Coatings Technology, 254 (2014) 244

[23] A. Laurino, E. Andrieu, J.P. Harouard, G. Odemer, J.C. Salabura, C. Blanc, Effect of corrosion on the fatigue life and fracture mechanisms of 6101 aluminum alloy wires for car manufacturing applications, Materials and Design, 53 (2014) 236-249

[24] A. Chemin, D. Spinelli, W. Bose Filho, C. Ruchert, Corrosion fatigue crack growth of 7475 T7351 aluminum alloy under flight simulation loading, Procedia Engineering, 101 (2015) 85-92

[25] M. Guerin, J. Alexis, E. Andrieu, C. Blanc, G. Odemer, Corrosion-fatigue lifetime of Aluminum-Copper-Lithium alloy 2050 in chloride solution, Materials and Design, 87 (2015) 681-69

[26] P. Hu, Q. Meng, W. Hu, F. Shen, Z. Zhan, L. Sun, A continuum damage mechanics approach coupled with an improved pit evolution model for the corrosion fatigue of aluminum alloy, Corrosion Science, 113 (2016) 78-90

[27] C.Q. Wang, J.J. Xiong, R.A. Shenoi, M.D. Liu, J.Z. Liu, A modified model to depict corrosion fatigue crack growth behavior for evaluating residual lives of aluminum alloys, International Journal of Fatigue, 83 (2016) 280-287

[28] B. Priet, G. Odemer, C. Blanc, K. Giffard, L. Arurault, Effect of new sealing treatments on corrosion fatigue lifetime of anodized 2024 aluminum alloy, Surface and Coating Technology, 307(A) (2016) 206-219

[29] Y. Chen, J. Zhou, Ch. Liu, F. Wang, Effect of pre-deformation on the pre-corrosion multiaxial fatigue behaviors of 2024-T4 aluminum alloy, International Journal of Fatigue, 108 (2018) 35-46

[30] A. Leon, E. Aghio, Effect of surface roughness on corrosion fatigue performance of AlSi10Mg alloy produced by Selective Laser Melting (SLM), Materials Characterization, 131 (2017) 188-194

[31] Y. Chen, Ch. Liu, J. Zhou, X. Wang, Multiaxial fatigue behaviors of 2024-T4 aluminum alloy under different corrosion conditions, International Journal of Fatigue, 98 (2017) 269-278

[32] S.R. Arunachalam, S.E.G. Dorman, R.T. Buckleya, N.A. Conrad, S.A. Fawaz, Effect of electrical discharge machining on corrosion and corrosion fatigue behavior of aluminum alloys, International Journal of Fatigue, 111 (2018) 44-53

[33] Z. Yea, D. Liu, X. Zhang, Z. Wu, F. Long, Influence of combined shot peening and PEO treatment on corrosion fatigue behavior of 7A85 aluminum alloy, Applied Surface Science, 486 (2019) 72-79

[34] Y. Chen, Ch. Liu, J. Zhou, F. Wang, Effect of alternate corrosion factors on multiaxial low-cycle fatigue life of 2024-T4 aluminum alloy, Journal of Alloys and Compounds, 772 (2019) 1-14

[35] R.I. Rodriguez, J.B. Jordon, P.G. Allison, T. Rushing, L. Garcia, Corrosion effects on fatigue behavior of dissimilar friction stir welding of high-strength aluminum alloys, Materials Science and Engineering A, 742 (2019) 255-268

[36] R.K. Mishra, Study the effect of pre-corrosion on mechanical properties and fatigue life of aluminum alloy 8011, Materials Today: Proceedings, 25(4) (2020) 602-609

[37] Y. Huang, X. Ye, B. Hu, L. Chen, Equivalent crack size model for pre-corrosion fatigue life prediction of aluminum alloy 7075-T6, International Journal of Fatigue, 88 (2016) 217-226

[38] M. Azadi, H. Aroo, Temperature effect on creep and fracture behaviors of nano-sio2-composite and alsi12cu3ni2mgfe aluminum alloy, International Journal of Engineering, 33(8) (2020) 1579-1589

[39] S.H. Juang, L.J. Fan, H.P.O. Yang, Influence of preheating temperatures and adding rates on distributions of fly ash in aluminum matrix composites prepared by stir casting, International Journal of Precision Engineering and Manufacturing, 16 (7) (2015) 1321-1327

[40] M. Zolfaghari, M. Azadi, M. Azadi, Characterization of high-cycle bending fatigue behaviors for piston aluminum matrix SiO2 nano-composites in comparison with aluminum-silicon alloys, International Journal of Metalcasting, 15 (2020) 152-168

[41] H. Aroo, M.S.A. Parast, M. Azadi, M. Azadi, Investigation of effects of nano-particles, heat treatment process and acid amount on corrosion rate in piston aluminum alloy using regression analysis, 11th International Conference on Internal Combustion Engines and Oil, Tehran, Iran (2020) (in Persian)

[42] K. Sasaki, T. Takahashi, Low cycle thermal fatigue and microstructural change of AC2B-T6 aluminum alloy, International Journal of Fatigue, 28 (3) (2006) 203-210

[43] Metallic materials-rotating bar bending fatigue testing, Standard No. ISO-1143, ISO International Standard (2010)

[44] M.J. Khameneh, M. Azadi, Evaluation of high-cycle bending fatigue and fracture behaviors in EN-GJS700-2 ductile cast iron of crankshafts, Engineering Failure Analysis, 85 (2018) 189-200

[45] M. Azadi, H. Aroo, Creep properties and failure mechanisms of aluminum alloy and aluminum matrix silicon oxide nano-composite under working conditions in engine pistons, Material Research Express, 6 (2019) 115020

[46] F. Zainon, K. Rafezi Ahmad, R. Daud, Effect of heat treatment on microstructure, hardness and wear of aluminum alloy 332, Applied Mechanics and Materials, 786 (2015) 18-22

[47] L. Han, Y. Sui, Q. Wang, K. Wang, Y. Jiang, Effects of Nd on microstructure and mechanical properties of cast Al-Si-Cu-Ni-Mg piston alloys, Journal of Alloys and Compounds, 695 (2017) 1566-1572

[48] A. Humbertjean, T. Beck, Effect of the casting process on microstructure and lifetime of the Al-piston-alloy AlSi12Cu4Ni3 under thermo-mechanical fatigue with superimposed high-cycle fatigue loading, International Journal of Fatigue, 53 (2013) 67-74

[49] M. Mollaei, M. Azadi, H. Tavakoli, A parametric study on mechanical properties of aluminum-silicon/SiO_2 nano-composites by a solid-liquid phase processing, Applied Physics A, 124 (2018) 504

[50] H.K. Issa, Taherizadeh, A. Maleki, A. Ghaei, Development of an aluminum/amorphous nano-SiO_2 composite using powder metallurgy and hot extrusion processes, Ceramics International, 43 (2017) 14582-14592

[51] G.F. Vander Voort, Metallography and Microstructures, sixth ed., ASM International, 2004

[52] Y. Li, Y. Yang, Y. Wu, L. Wang, X. Liu, Quantitative comparison of three Ni-containing phases to the elevated-temperature properties of Al-Si piston alloys, Material Science Engineering A, 527 (26) (2010) 7132-7137

[53] M.J. Sharifı, M. Azadi, M. Azadi, Fabrication of heat-treated nano-clay-composite for improving high-cycle fatigue properties of AlSiCu aluminum alloy under stress-controlled fully-reversed bending loads, Part C: Journal of Mechanical Engineering Science, (2020)

[54] J. Liu, Q. Zhang, Z. Zue, Y. Xiong, F. Ren, A. Volinsky, Microstructure evolution of Al-12Si-CuNiMg alloy under high temperature low cycle fatigue. Materials Science Engineering A, 574 (2013) 186-190

[55] G. Zhang, J. Zhang, B. Li, W. Cai, Double-stage hardening behavior and fracture characteristics of a heavily alloyed Al-Si piston alloy during low-cycle fatigue loading, Materials Science Engineering A, 561 (2013) 26-33

[56] M. Arab, M. Azadi, O. Mirzaee, Effects of manufacturing parameters on the corrosion behavior of Al-B4C nanocomposites, Materials Chemistry and Physics, 253 (2020) 123259

[57] M.S.B. Selamat, Corrosion behavior of SiCp/6061 Al metal matrix composites in chloride solutions, Advanced Performance Materials, 3 (1996) 183-204

[58] Z. Li, N. Limodin, A. Tandjaoui, P. Quaegebeur, J.F. Witz, D. Balloy, Influence of Fe content on the damage mechanism in A319 aluminum alloy: Tensile tests and digital image correlation, Engineering Fracture Mechanics, 183 (2017) 94-108

Figures

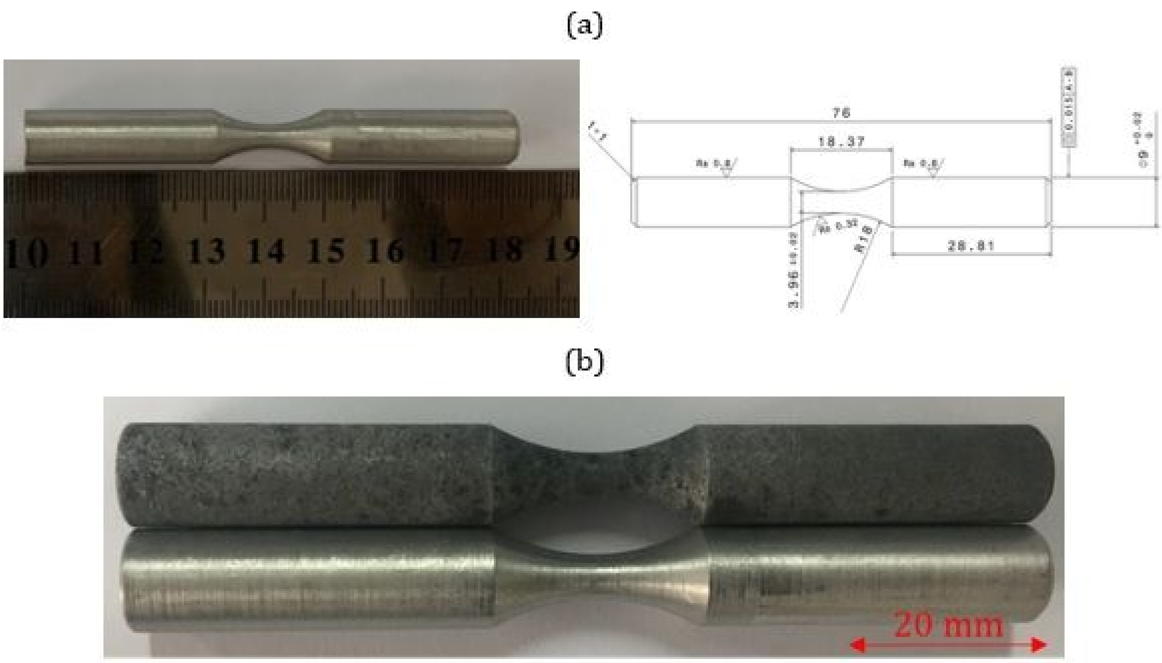

Figure 1

The specimen of fatigue testing including (a) the specimen geometry (b) the specimen before and after the pre-corrosion process

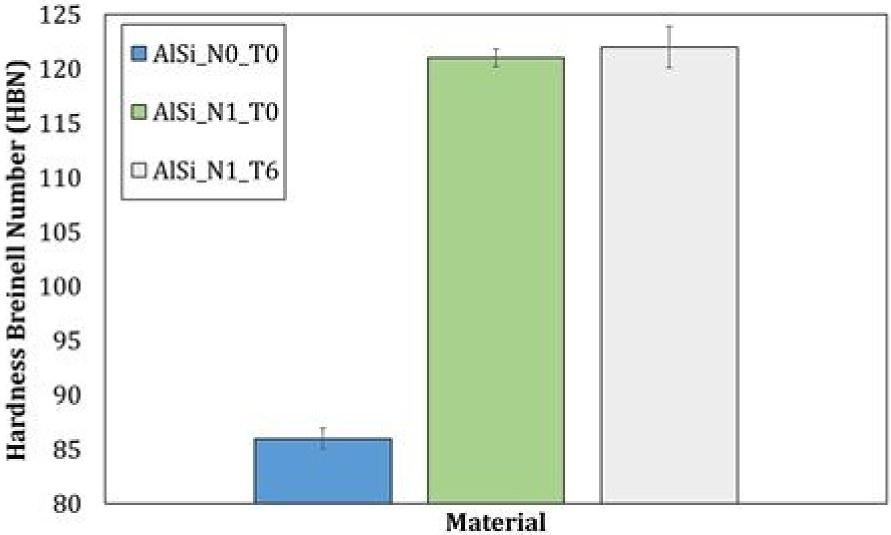

Figure 2

Comparative results of the hardness test

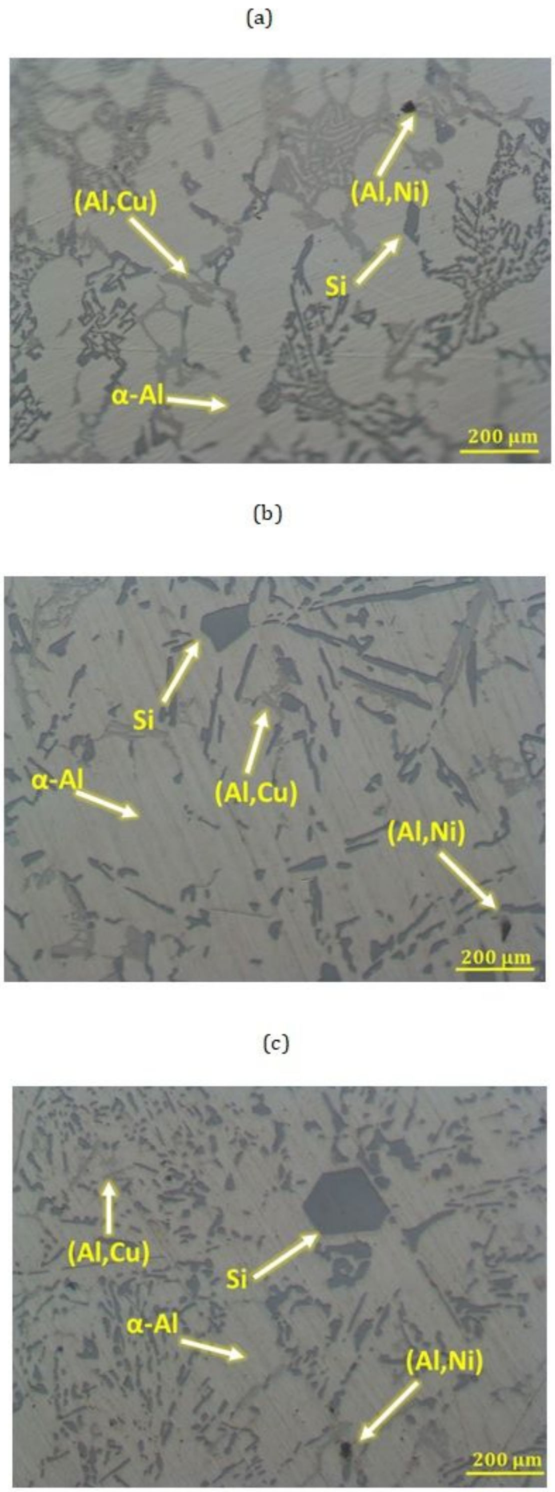

Figure 3

The material microstructure before fatigue testing, including (a) the aluminum-silicon alloy, (b) the nano-composite and (c) the heat-treated nano-composite

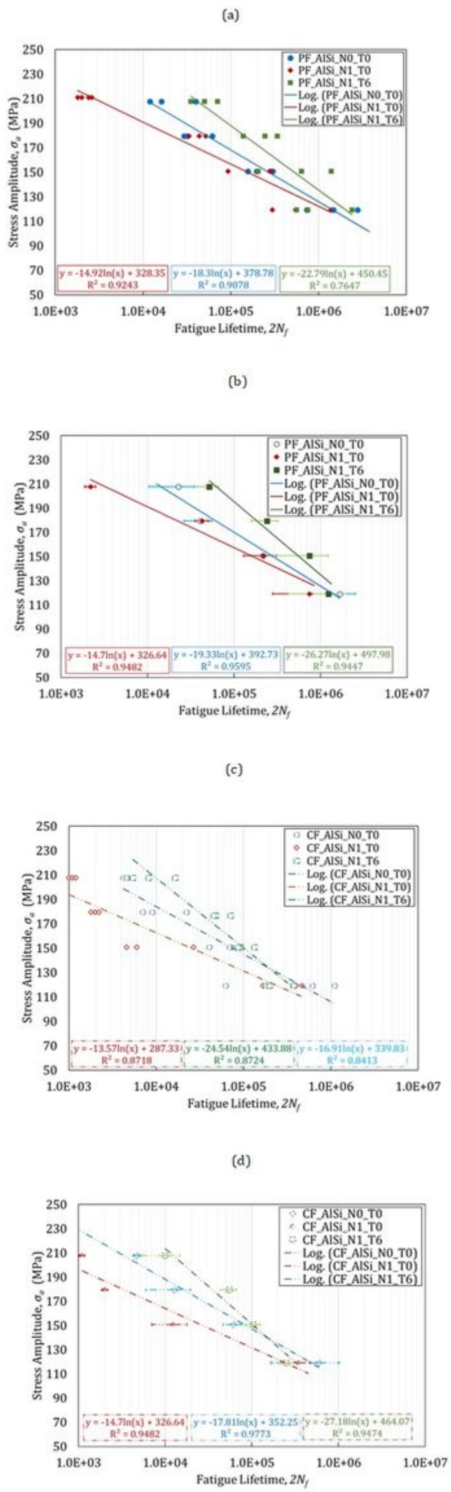

Figure 4

Stress-lifetime curves for all studied materials for (a) all fatigue data, (b) averaged fatigue data points, (c) all corrosion-fatigue data and (d) averaged corrosion-fatigue data

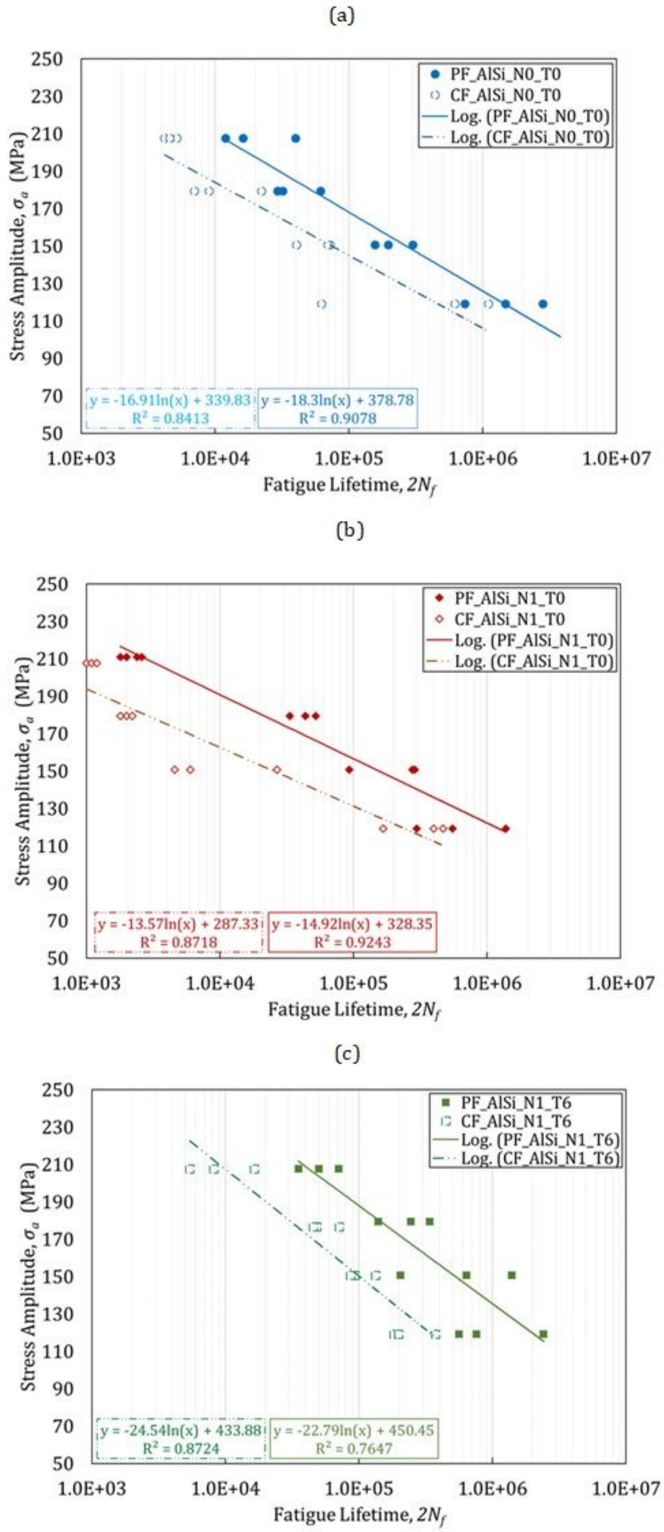

Figure 5

Stress-lifetime curves for fatigue and corrosion-fatigue data for (a) the piston aluminum-silicon alloy, (b) the nano-clay-composite and (c) the heat-treated nano-clay-composite

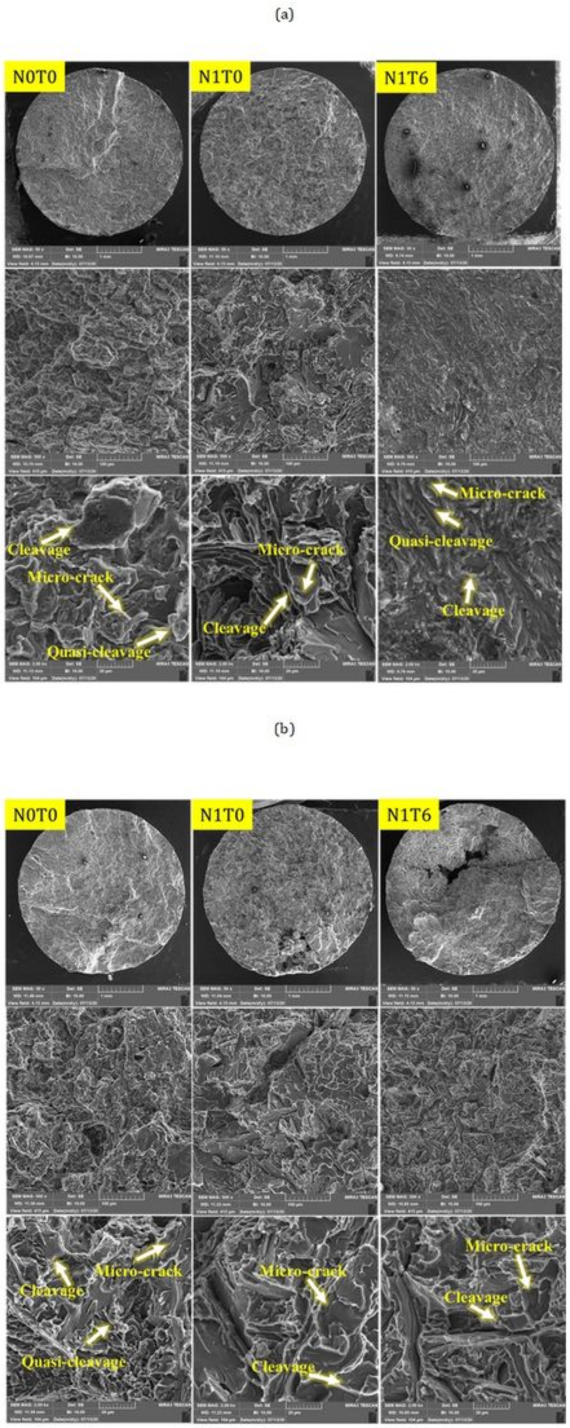

Figure 6

The FE-SEM image of the fracture surface after fatigue testing for piston aluminum alloys with and without reinforcements under (a) fatigue and (b) corrosion-fatigue loadings

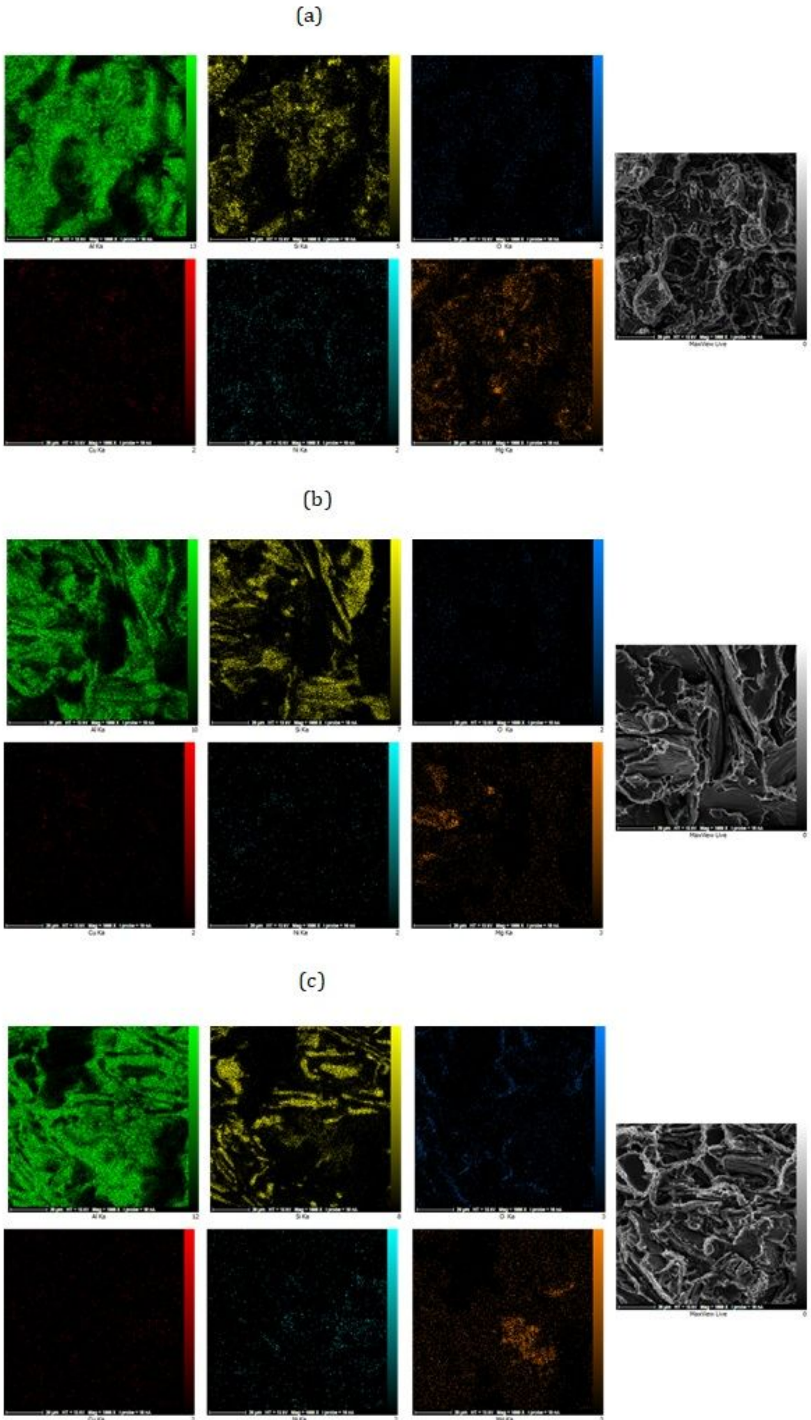

Figure 7

The EDX map of the fracture surface after fatigue testing including (a) the piston aluminum alloy (b), the piston aluminum alloy reinforced with nano-particles, and (c) the piston aluminum alloy reinforced with both nano-particles and the heat-treatment

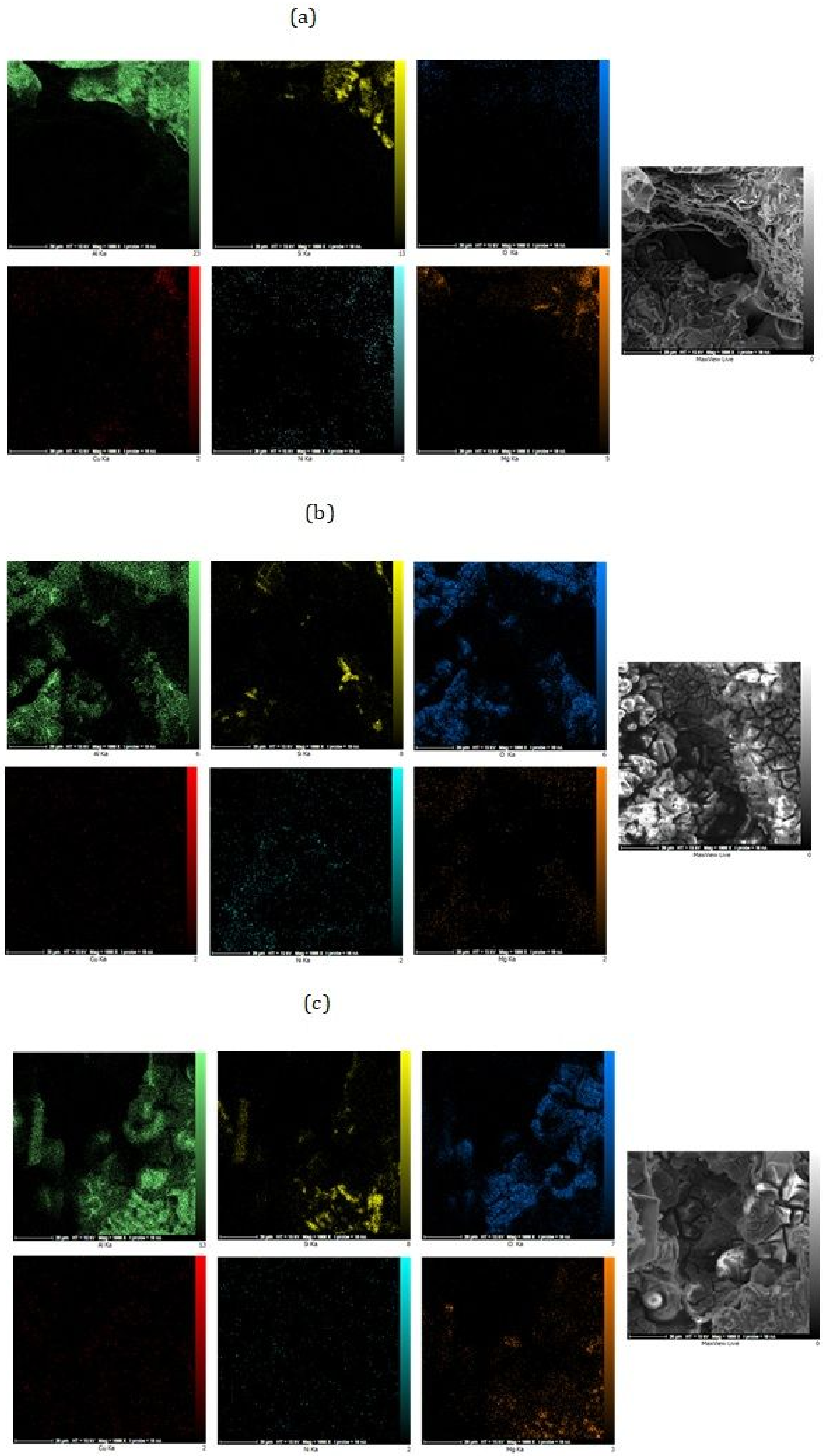

Figure 8

The EDX map of the fracture surface after corrosion-fatigue testing including (a) the piston aluminum alloy (b), the piston aluminum alloy reinforced with nano-particles, and (c) the piston aluminum alloy reinforced with both nano-particles and the heat-treatment